Understanding phase equilibria in high-entropy alloys: II. Atomic-scale study of incorporation of metallic elements in Cr carbides – Application to equilibrium with AlCrFeMnMo

Rémy Besson

Understanding phase equilibria in high-entropy alloys: II. Atomic-scale study of incorporation of metallic elements in Cr carbides – Application to equilibrium with AlCrFeMnMo

Remy Besson

Understanding phase equilibria in high-entropy alloys: II. Atomic-scale study of incorporation of metallic elements in Cr carbides – Application to equilibrium with AlCrFeMnMo

R. Besson

Univ. Lille, CNRS, INRAE, Centrale Lille, UMR 8207 - UMET - Unité Matériaux et Transformations, F-59000 Lille, France

ARTICLE INFO

Article history:
Received 11 February 2021
Received in revised form 23 March 2021
Accepted 9 April 2021
Available online xxx

Keywords
Density functional theory
Carbides
Phase equilibria
Multiprincipal metallic solid solutions

ABSTRACT

Using atomic-scale first-principles energy calculations, we describe a methodology allowing to investigate the effect of metallic elements in frequently encountered $Cr_{23}C_6$ carbides, and its application to the equilibrium between $Cr_{23}C_6$ and AlCrFeMnMo high-entropy solid solutions. Our study reveals the importance of taking properly into account the effect of interstitial C in $Cr_{23}C_6$, since the latter is found to have a key-influence on the thermodynamics of the compound. Moreover, it emphasizes clear-cut trends as regards the propensity of the various metallic elements to penetrate the carbide. Finally, it illustrates the role of the chemical potentials in the high-entropy solid solution, since the latter are the key-quantities controlling the composition of $Cr_{23}C_6$. The tractability of the approach described here should allow easy applications to similar cases, including other chemically complex solid solutions, as well as various second-phase particles (carbides, nitrides, oxides, borides…) unavoidably formed during elaboration processes.

1. Introduction

New routes of explorations are currently being opened in metallurgy, due to the emergence of multi-principal-element metallic alloys, noticeably the so-called "high-entropy alloys" (HEAs). HEAs nowadays offer a wide, still largely unknown, class of materials with intriguingly outstanding thermochemical and mechanical properties, ranging from high strength [1] to corrosion or creep resistance [2,3]. Moreover, in connection with their reputedly high entropy, the stability of HEAs is strongly dependent on thermodynamic criteria [4]. Thermodynamics thus determines, not only the main HEA phase, i.e. the multi-principal-element metallic solid solution (s.s.) itself, but also the various surrounding phases, which are in equilibrium with this s.s., and are usually formed – be they desired or not – during the elaboration processes. It is thus of primary importance to get a better understanding of the physical mechanisms controlling the formation of these phases.

Among the various kinds of HEAs currently under investigations [5], the AlCrFeMnMo system has been paid little attention up to now [6]. Nevertheless, recent experimental studies [7] have pointed out the interest of exploring this quinary system, to elaborate single-phase disordered alloys with the body-centered cubic (bcc) structure and good properties for coatings with various thicknesses (between 100 nanometers and 100 μm). In addition to (un)desired metallic elements, oxygen and carbon are also frequently detected in HEA samples, whatever the respective roles of the solid and liquid states in the elaboration. As for carbon, the origin of this element can often be traced back to the use of organic solvents required during the process. It is worth mentioning the difficulties with the detection of carbon by experimental means in HEA solid solutions, hence a fortiori with considering quantitative measurements on such light elements. In close connection with this poorly controlled presence of C, the behaviour of practically important second-phase particles in chemically complex environments involving many concentrated metallic elements is almost totally unknown. As concerns particularly AlCrFeMnMo, a major concern was found [7] to be the unexpected presence of multi-element carbides, especially $Cr_{23}C_6$–type compounds having a face-centered cubic structure with a large unit cell (~10 Å). Although well-known in various metallurgical fields (stainless steels…), the role of these carbides is somewhat more difficult to understand in the context of HEAs. A key-issue in this direction would be provided by the elucidation of the unknown features of their equilibrium with the main multimetallic s.s., which has direct consequences on the composition of the phases. Interestingly, previous experiments on AlCrFeMnMo [7] have suggested that other metallic elements, such as Mo, might play a special role in $Cr_{23}C_6$–type carbides, leading to the simultaneous formation of several carbide phases, each of which may contain either Cr or Mo as major metallic element.

Trying to interpret these experimental facts, one is faced with a rather intricate situation: (i) $Mo_{23}C_6$ is currently not referenced as a specific phase in crystallographic databases [8], which strikingly contrasts with the common crystal structure referenced for $Cr_{23}C_6$ and $Mn_{23}C_6$, (ii) several attempts to evaluate and compare the relative ther-

modynamic stabilities of Cr and Mo carbides have been carried out [9,10], leading to the conclusion that $Mo_{23}C_6$ should have a lower free energy than $Cr_{23}C_6$ below 700 °C. However, such arguments can obviously not be employed as such, in order to infer any conclusion about these relative stabilities, due to the fact that Cr and Mo carbides do not have the same composition. In steels containing Cr and Mo, it is also a well-known fact that such carbides occur in the form $M_{23}C_6$ with M = (Cr,Fe,Mo) [9]. On the whole, there remains considerable uncertainty as regards the compositions adopted by $Cr_{23}C_6$-type carbides in usual steel environments, due to the strong trend of these compounds to incorporate other elements such as Fe, Co or Mo, and the reasons for this remarkable feature thus remain to be determined. Investigating the meaning and validity of $M_{23}C_6$ as a reliable chemical formula for these carbides becomes even more critical in environments with higher chemical complexity, such as HEA multimetallic concentrated alloys. In particular, since the HEA considered in our work also involves Al and Mn, this system provides a good opportunity to increase our knowledge of the mechanisms underlying the respective occurrence of, and possible competition between, $(Cr,Fe,Mo)_{23}C_6$ and $Mn_{23}C_6$ carbides, as well as to clarify the possible role of seemingly "spectator" elements such as Al in these phase transformations.

In this context, the interest of theoretical approaches coupled to numerical simulations is doubtless, since state-of-the-art experimental measurements still hardly make it possible to grasp with accuracy (i) the presence of the various metallic elements in carbides, (ii) the behaviour of C in these miscellaneous metallic environments. In this respect, the use of atomic-scale approaches is appealing, since macroscopic frameworks (in particular, Calphad-type phenomenological thermodynamic calculations), although they provide a more tractable frame to discuss phase stability and equilibria, still suffer from a critical lack of reliable input data when tackling multi-element systems such as HEAs. While ab initio simulations on AlCrFeMnMo bcc s.s. are still lacking, several works [11,12] have used this methodology to tackle the issue of $M_{23}C_6$ stability. While these works consider the interesting case of Fe substitution in carbides, the scope of their conclusions however remains somewhat restricted, due to the use of specific energy references strongly different from those relevant for HEAs.

The aim of our work is to use atomic-scale simulations and modellings to investigate the features of the thermodynamic equilibria arising between the bcc s.s. and $M_{23}C_6$ carbides during the elaboration of HEAs from the quinary AlCrFeMnMo system, thus contributing to remove ambiguities, regarding the methodological aspects as well as the conclusions, about the thermodynamic stability of $M_{23}C_6$ carbides. To this aim, ab initio energy calculations and thermodynamic modellings of the chemical potentials (section II) will be employed, to investigate the properties of the $M_{23}C_6$ carbide (section III), thus providing information of the conditions of equilibrium between both phases, and allowing to discuss their implications for the elaboration of AlCrFeMnMo HEAs (section IV).

2. Methods

2.1. Ab initio calculations

For the atomic-scale modelling of the carbide, due to the relatively large size of the $Cr_{92}C_{24}$ unit cell, the required point defect calculations were carried out on a supercell identical to this unit cell. The required ab initio calculations were performed with the VASP (Vienna Ab initio Simulation Package) software [13], using the Projector Augmented Wave mode [14] and the GGA approximation with the PBE functional [15,16]. The pseudopotentials used contained 6 and 4 valence electrons for Cr and C, and (3, 8, 7, 6) valence electrons for (Al, Fe, Mn, Mo) respectively. The energy cutoff for the plane wave expansion was chosen equal to 560 eV throughout, and the k-point mesh was of Monkhorst-Pack [17] type with a 6×6x6 grid. These cutoff and k-point values ensured reasonable accuracy for all total energies. A first-order Methfessel-Paxton [18] smearing scheme was used, with a smearing width of 0.2 eV. All calculations were spin-polarized (collinear mode), and earlier studies [19] suggested to use zero initial magnetic moments for all species, except (i) Fe atoms for which the usual value $\mu_{mag}(Fe) = 2.2\ \mu_B$ was specified, and (ii) Mn for which earlier investigations suggested to test several possibilities (-2, 0 or $+2\ \mu_B$) for the Mn initial moment [19], the lowest total energy value after relaxation being retained for each defect. In all cases, the structural optimization included full supercell relaxation, namely local atomic relaxations as well as supercell size and shape, in order to ensure zero local stress.

2.2. Chemical potentials in carbide from independent-point-defect approximation

The independent-point-defect approximation (IPDA), already described in detail elsewhere [20], offers a convenient way to investigate the properties of ordered compounds for moderate deviations from stoichiometry. As a major advantage, the good tractability of this approach allows significant versatility, making it a valuable tool for investigations in multicomponent environments. More precisely, in the present case, the IPDA framework was employed to study the response of $Cr_{23}C_6$ (chromium being the base metallic element in the carbide) to the addition of the other elements (Al, Fe, Mn, Mo) induced by the presence of the multimetallic s.s. It is worth emphasizing that the IPDA is most conveniently formulated in the grand canonical framework, the carbide properties being then controlled by the chemical potentials. Since the latter are imposed by the surrounding s.s., this provides a direct route to explore the features of the equilibrium between the s.s. and the carbide.

The IPDA key-parameters are the grand canonical (GC) energies of the various point defects occurring in the compound [20]:

$$E_{GC}(d) = E(d) - E_0 \tag{1}$$

$E(d)$ and E_0 being respectively the total energies for a system with a single isolated point defect of type d, and for the reference undefected system. In the present case, the point defects considered belong to two distinct categories, namely:

1) the intrinsic point defects of $Cr_{23}C_6$, including Cr and C antisites and vacancies, and possibly interstitial C;
2) the extrinsic point defects, due to the presence of the substitutional addition elements (Al, Fe, Mn, Mo) on sites normally occupied by Cr.

The $Cr_{23}C_6$ carbide being characterized by a set of five distinct sublattices, i.e. {4a, 8c, 32 f, 48 h} sites for Cr and 24e sites for C, each point defect will be specified throughout, as usually done, by its chemical species and site label, hence the sets of intrinsic {C_{4a}, C_{8c}, $C_{32\,f}$, $C_{48\,h}$, Vac_{4a}, Vac_{8c}, $Vac_{32\,f}$, $Vac_{48\,h}$, Cr_{24e}, Vac_{24e}} (Vac = vacancy), and extrinsic {X_{4a}, X_{8c}, $X_{32\,f}$, $X_{48\,h}$, X_{24e}} (X = Al, Fe, Mn, Mo) point defects. In addition, the possible role of interstitial sites (restricted to C occupancy for reasons of atomic size) was also considered, giving rise to additional possibilities of defects caused by interstitial carbon.

3. Results

3.1. Elucidating carbon behaviour in $Cr_{23}C_6$ carbide

Considering the HEA-type AlCrFeMnMo bcc s.s., our main purpose consists in exploring the properties of the equilibrium between this s.s. and carbides with the well-known $Cr_{23}C_6$ structure, since the latter were recurrently observed in experiments on this quinary metallic system. To help bring some elements of response to these experimental issues, the chemical potentials are the key-quantities, since they deter-

mine the compositions of the phases in equilibrium. Due to the complexity induced by the five-sublattice and large-unit cell crystal structure of $Cr_{23}C_6$, intricacy further enhanced, in multimetallic environments such as HEAs, by the possible presence of other metallic elements on these sublattices, it is reasonable to choose for $Cr_{23}C_6$ some sufficiently tractable modelling framework. The IPDA approach followed here fulfills these requirements, since it allows taking into account, in a handsome way, the role of the addition elements brought by the surrounding metallic s.s. For reasons of atomic size, the possibility for the metallic elements to occupy interstitial sites was not considered. As mentioned above, the key-quantities for $Cr_{23}C_6$ when using IPDA are the point defect grand canonical energies: for vacancy and antisite defects (the usual defects in metallic ordered compounds), these quantities are thus listed in the first three columns of Table 1. Moreover, the presence of carbon makes it highly probable that this element may occupy interstitial sites. Inspection of the space group of $Cr_{23}C_6$ (n°225 Fm-3 m) suggests to include two types of interstitial sites, namely 4b and 24d, since both have well-defined and simple positions in the unit cell. The GC energies for these supplementary C defects are thus presented in Table 2, which shows that all E_{GC} are found to be positive, except those pertaining to interstitial C. It should however be noted that nothing can be inferred from these "raw" E_{GC} values, which then have to be used as input in the IPDA modelling, as described in the following. The thermodynamic behaviour of $Cr_{23}C_6$ results from an overall balance between the energy contributions of the various defects.

Table 1
Grand canonical energies E_{GC} (eV) of (Cr, C, Vac = vacancy) intrinsic and (Al, Fe, Mn, Mo) addition point defects in $Cr_{23}C_6$ (including some optimization on the initial Mn magnetic moment for Mn defects, see text). All calculations were performed with the VASP software.

	Cr	C	Vac	Al	Fe	Mn	Mo
4a	–	1.912	10.186	5.172	0.638	0.071	-0.660
8c	–	2.878	12.476	5.838	1.581	0.519	-1.659
32 f	–	3.813	11.596	6.224	1.467	0.459	-0.672
48 h	–	4.584	12.081	6.165	1.352	0.404	-0.952
24e	3.445	–	11.477	9.485	3.672	3.160	4.469

Table 2
Grand canonical energies (eV) of interstitial C point defects in $Cr_{23}C_6$, for the various sites chosen from Fig. 2, as obtained from ab initio calculations. It should be noted that, due to the particular choices of (x,y,z), the multiplicities of sites 96j1, 96j2 and 96k are 24, 48 and 32 respectively, instead of the expected common value 96 (all calculations were performed with the VASP software).

Interstitial site	E_{GC} for carbon
4b (1/2 1/2 1/2)	-6.749
24d (0 1/4 1/4)	-6.112
48 g (x 1/4 1/4, x = 1/8)	-7.904
48i (1/2 y y, y = 1/8)	-3.816
96j1 (0 y z, y = 1/2, z = 3/8)	-7.023
96j2 (0 y z, y = z = 5/12)	-6.450
96k (x x z, x = z = 1/8)	-8.546

The basic valuable result from IPDA is the intrinsic point defect structure of the carbide, which is displayed on Fig. 1a for 800 K. In general, for any ordered compound, it is important to identify the type of dominant point defect required to accommodate each kind of off-stoichiometry, i.e. the so-called structural defects. For $Cr_{23}C_6$, while C depletion is due to vacancies on 24e sites, C excess is found to be mainly due to antisite C atoms on 4a sites, whereas the amount of Cr vacancies on 4a sites cannot exceed a much lower level. This substitution of a metal by a non-metal could probably be explained by the complex local environments in the carbide, possibly lowering the energy cost of C antisites (second column, rows 1–4 in Table 1). Here the role of interstitial C surprisingly appears to be minor: C_{4b} is much more favourable than C_{24d}, but the energetics of C_{4b} is unable to modify strongly the outcome of the competition between antisite and interstitial C atoms. As a second striking feature, the presence of four Cr sublattices is responsible for the large contrast between both sides of stoichiometry, due to the successive filling, within a moderate range of 10% C enrichment, of all 4a, and then all 8c sites, with C. Interestingly, a moderate C-rich off-stoichiometry (a few at% excess C) is also found to gradually activate the C-filling on 32 f, and then 48 h, sites, but the required level of C excess, for this secondary effect to become important, may lie beyond the IPDA validity domain. On the whole, in this five-sublattice picture of $Cr_{23}C_6$, the C-rich side thus shows a rather complex behaviour, illustrated for instance by the non-monotonous profile of 4a Cr vacancies, this feature resulting from the vicinity in composition space of a hypothetical $Cr_{22}C_7$ (x_C = 24%) variant in which all 4a sites should be filled with C.

This predicted behaviour of $Cr_{23}C_6$, noticeably the negligible influence of interstitial C, can hardly be checked by experiments. However, it is sufficiently unexpected to suggest that other interstitial sites may have been overlooked and, though less symmetrical than 4b and 24d,

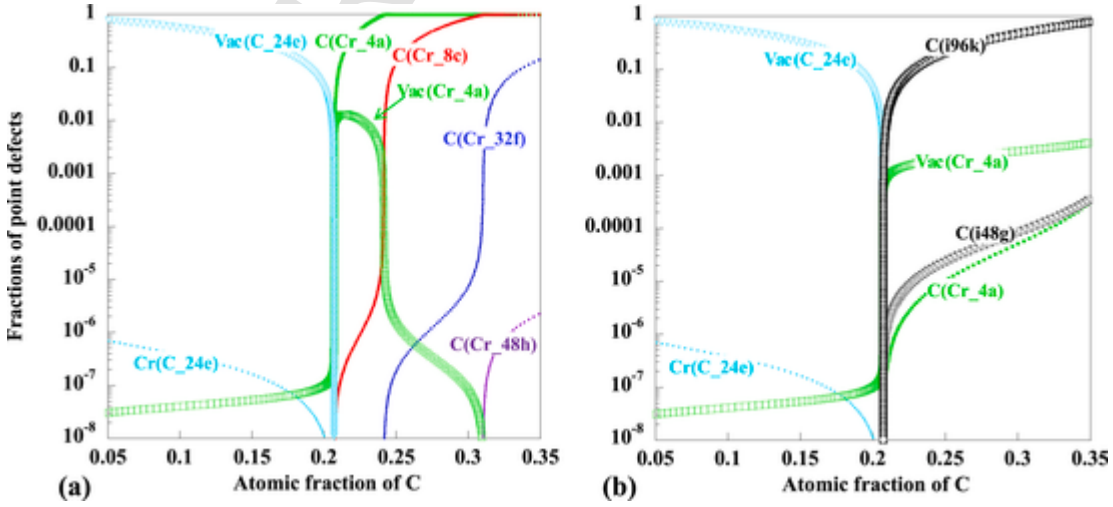

Fig. 1. From ab initio energetics and IPDA thermodynamics, amounts of intrinsic point defects in $Cr_{23}C_6$ at 800 K (a) allowing only 4b and 24d sites for interstitial C, (b) taking into account the whole set of carbon interstitial sites depicted in Fig. 2 and Table 2.

could be active in this compound. Indeed, the properties of the Fm-3 m space group indicate that other interstices are available beyond 4b and 24d, namely 48 g, 48i, 96j and 96k (Table 2). When selecting these additional sites, some choice of coordinate has to be made, depending on the precise structure of the compound. As depicted on Fig. 2, this choice was carried out iteratively by visual inspection, by examining at each step the room available for the new probed site, in order to avoid any overlapping as well as any redundant choice. For 48 g sites located on directions of type x 1/4 1/4, Fig. 2a indicates that x = 1/8 is available, while y = 1/8 seems convenient for 48i on 1/2 y y directions (Fig. 2b). 96j positions of type 0 y z may lie within the whole (100) plane, and Fig. 2c suggests two possibilities, noted 96j1 and 96j2, at y = 1/2, z = 3/8 and y = z = 5/12. Finally, for 96k sites of type x x z lying within the (1−10) plane, Fig. 2d indicates that x = z = 1/8 is a reasonable choice.

The GC energies of C occupying these supplemental interstitial sites are listed in Table 2, which shows that 48 g, 96j1 and 96k are much more stable than the 4b and 24d sites chosen initially. Noticeably, the largest stability is found to occur for 96k, namely those sites with the lowest symmetry, followed by 48 g. This clearly illustrates the difficulty inherent to identifying the relevant point defects in compounds involving light elements sufficiently small to activate unexpected interstitial sites. As shown on Fig. 1b, including all interstitial sites of Table 2 in the IPDA calculation deeply modifies the predicted point defect structure of the carbide, which recovers a much simpler aspect. In particular, in agreement with experimental data, $Cr_{23}C_6$ indeed appears to be the central stoichiometry within a large composition window, the possibility of competing neighbour variants such as $Cr_{22}C_7$ being now ruled out. The point defect structure of the compound is monitored by interstitial C or C vacancies, the site occupancies of Cr atoms appearing largely unaffected by composition changes. The amounts of Cr and C antisites are small ($< 10^{-5}$ at 800 K), which seems satisfactory.

These trends on amounts of point defects can directly be translated into profiles of composition-dependent point defect formation energies. Maybe more clearly than Fig. 1, this representation (Fig. 3) emphasizes the critical effect of properly choosing the kinds of point defects to include into the IPDA thermodynamic formalism. In particular, allowing only 4b and 24d sites for interstitial C (Fig. 3a) entails a zero formation energy for C_{4a} defects (noted C_Cr4a on the figure) for surprisingly small C excess (~2 at%). The negative formation energies occurring beyond this moderate threshold are a hint of the inadequacy of the (4b;24d)-limited IPDA modelling. This hypothesis is indeed confirmed when including all kinds of interstitial sites for C (Fig. 3b): in the latter case, a satisfactory picture is recovered for the carbide, with positive defect formation energies for all point defects in a much larger off-stoichiometry range. Finally, it may also be recalled that the relative stabilities of point defects can directly be inferred from their formation energies, while comparing the E_{GC} energies (given in Table 1 and 2) for this purpose would be erroneous.

From the above described point defect properties, the IPDA formalism also conveniently allows to derive the thermodynamic properties of the carbide, which are of primary interest in the present context of equilibrium with multimetallic solid solutions. To calculate the compound formation free energy (Fig. 4a), references of −9.506 and −10 eV were used for Cr and C respectively, the former value corresponding to bcc Cr while the latter was chosen somewhat arbitrarily, though in a reasonable range. The compound stability for C-rich off-stoichiometry is significantly increased by including properly interstitial C. The same effect is also visible on the chemical potentials μ(Cr) and μ(C) (Fig. 4b), where the presence of all types of interstitials entails a shrinking of the μ domain associated to the stoichiometric compound. Nevertheless, since our analysis has revealed that the (4b;24d)-limited IPDA modelling of $Cr_{23}C_6$ is probably inadequate, it is displayed (open symbols in

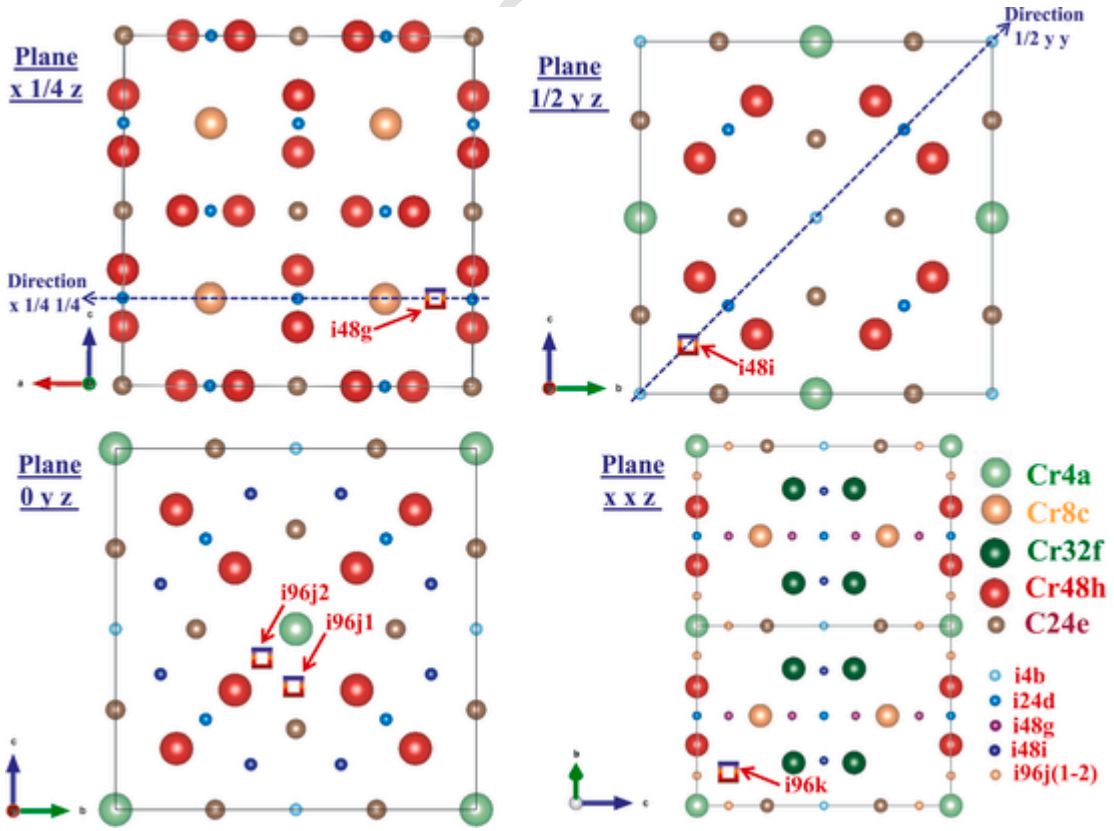

Fig. 2. Sketch of the various crystal planes relevant for successive identification of possible interstitial sites beyond (4b; 24d) in $Cr_{23}C_6$. On each figure, the open square depicts the new interstitial site probed at this step. The figure was realized using the VESTA (Visualization for Electronic and Structural Analysis) software [21].

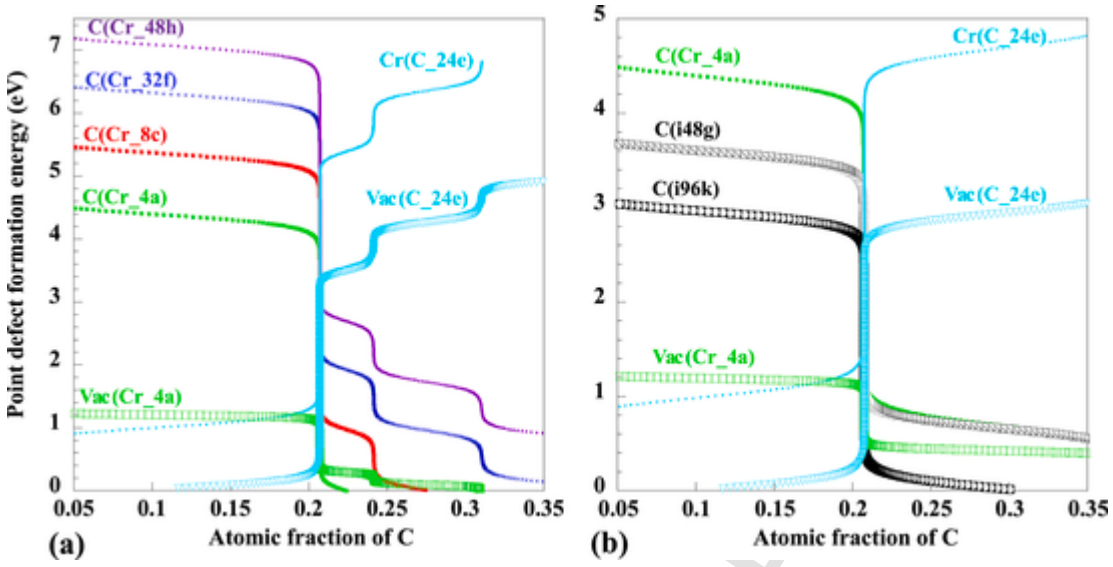

Fig. 3. From ab initio energetics and IPDA thermodynamics, formation energies of intrinsic point defects in $Cr_{23}C_6$ at 800 K (a) allowing only 4b and 24d sites for interstitial C, (b) taking into account the whole set of carbon interstitial sites (see Fig. 2 and Table 2).

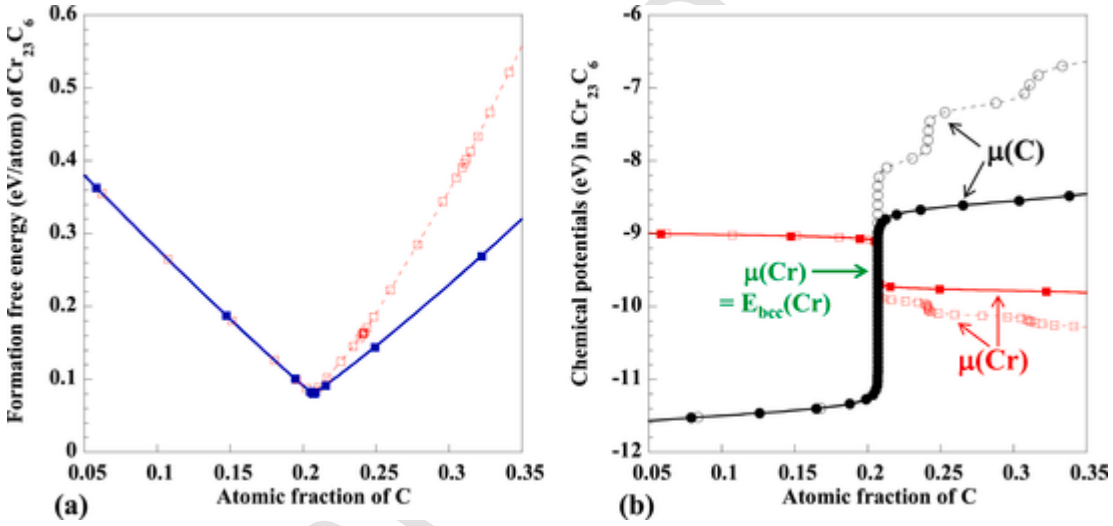

Fig. 4. (a) Formation free energy and (b) elemental chemical potentials (red squares = μ(Cr), black circles = μ(C)) for $Cr_{23}C_6$ at 800 K from ab initio IPDA. Both in figures (a) and (b), the results are displayed for interstitial C defects occupying either only (4b;24d) sites (open symbols) or all interstitial sites listed in Table 2 (full symbols). The green arrow on Figure (b) indicates the Cr chemical potential taken from Table 3.

Fig. 4) merely for purpose of methodological completeness, but this modelling should not be used further for the carbide. On the whole, the interest of this section devoted to a detailed IPDA study of $Cr_{23}C_6$ point defects and thermodynamics is twofold: (i) elucidating the role of C in this compound, via the identification of the relevant interstitial sites accessible to this light element, (ii) providing a sound basis for the derivation of the chemical potentials in $Cr_{23}C_6$, key-quantities when investigating the equilibrium between this compound and multi-principal-element HEA solid solutions.

3.2. Effect of metallic additions in $Cr_{23}C_6$ and equilibrium with AlCrFeMnMo solid solutions

As mentioned previously, the IPDA offers a convenient framework to investigate the response of the $Cr_{23}C_6$ carbide to multi-metallic environments such as encountered in high-entropy alloys. More precisely, it was shown elsewhere [20] that the IPDA formalism describing an ordered compound lends itself to tractable extensions that allow investigating the effects due to the incorporation of addition elements. This is especially relevant for the "grand canonical" formulation (not to be mixed up with the "grand canonical energies" required as input data) of the formalism, which is well adapted to situations in which the chemical potentials of the additions in the carbide can be considered as a priori known quantities, here through the multi-metallic-element s.s. characteristic of HEAs. In this context, the required input quantities are the GC energies of the various additions, which are listed in Table 1 for the case of substitutional metallic defects only. Interestingly, all values are found positive, except for Mo on Cr sites, but here again, as pointed out previously for intrinsic defects, no conclusion can be drawn from this feature, since the behaviour of each addition element in the carbide depends on the corresponding elemental chemical potential which reflects the equilibrium with the surrounding medium. For Mn defects, the possible influence of the initial Mn magnetic moment was considered, but this influence was found to be negligible, except in the case of Mn_{4a} defects, for which neglecting the residual Mn moment ~ 0.45 μ_B would entail a 60 meV excess GC energy. As regards the Cr sub-

lattices, Table 1 indicates that site preferences should be 4a for Al, Fe, Mn, and 8c for Mo, but more detailed investigations below will show that this analysis of site preference based solely on GC energy comparison may be oversimplified. Moreover, as a first approach, since a detailed knowledge of the temperature- and composition-dependent metallic chemical potentials in a typical HEA s.s. deserve investigations beyond the scope of the present work, the chemical potentials of Al, Fe, Mn and Mo in the surrounding s.s. were chosen to be equal to the energies of these pure elements in the bcc structure under zero pressure (Table 3). In the case of bcc AlCrFeMnMo HEAs, other studies [22] suggest that this choice for the metallic chemical potentials should be a reasonable assumption.

From this energetics, the overall effect of C content on the various addition point defects can be studied, and is presented on Fig. 5a. It shows that the occupancy of the carbon 24e sublattice is negligible ($< 10^{-7}$, hence not visible on Fig. 5a) for Al and Mo whatever the carbon content, whereas some significant presence of Fe and Mn on 24e is noted in the C-depleted carbide, this behaviour being close to that already obtained for Cr (Fig. 1b). Fig. 5a confirms that Al and Fe primarily occupy 4a sites, whereas for Mn the conclusion is slightly different from that previously drawn from GC energies: as an effect of element competition on the various sublattices, Mn turns out to occupy preferentially 32 f and 48 h sites, while 4a occupancy remains lower, and is widely composition-independent (which is true for all elements). From these properties of addition point defects, the influence of C content on the overall penetration of addition elements in the carbide can easily be inferred, as depicted on Fig. 5b. It shows that incorporation of Fe is always negligible, while the carbide should accept limited amounts of Al and Mo. As regards Mn, the IPDA suggests for this element a much different behaviour, with the possibility of massive incorporation into $Cr_{23}C_6$ under specific conditions. Of course, this conclusion has to be taken with some precaution, due to the high spatial density of the 32 f and 48 h sites involved in this process, which may conflict with the hypothesis of non-interacting point defects founding the IPDA. Nevertheless, this probably points out some reliable trend of Mn in $Cr_{23}C_6$, which should be taken into account in the interpretation of experiments on the s.s.-carbide two-phase system. Noticeably, our analysis qualitatively agrees with the fact that the $Mn_{23}C_6$ carbide, with the same Fm-3 m space group as $Cr_{23}C_6$ (but possibly ill-identified atomic positions), is also referred to in the literature. On the whole, our study indicates that, in this AlCrFeMnMo concentrated multimetallic environment, the carbide should more realistically be viewed - at least - as $(Cr,Mn)_{23}C_6$, or even as $(Cr,Al,Mn,Mo)_{23}C_6$. It also shows the existence of a critical amount of C in the s.s. beyond which Mn should massively replace Cr in the carbide.

Table 3
Reference energy (eV/atom) of each metallic element in the bcc structure with its equilibrium zero pressure lattice parameter. All calculations were performed with the VASP software.

	Cr	Al	Fe	Mn	Mo
E(bcc)	-9.506	-3.648	-8.306	-8.877	-10.944

4. Discussion

The approach described in this work offers a tractable way to evaluate the behaviour of second-phase particles such as carbides in multi-element environments, the latter being increasingly investigated in materials science, for instance in the framework of high-entropy alloys. While it offers a sound basis, resting on the point-defect thermodynamics of a compound, its main limitation comes from the fact that possible interactions between intrinsic and/or addition point defects are neglected. This limitation could be partially overcome by considering more elaborate descriptions of the compound, in particular those relying on the cluster expansion (CE) formalism [23] encompassing larger composition domains. However, due to the rapidly increasing complexity of such descriptions with the number of elements involved, it is likely that the information obtained from the IPDA preliminary approach presented above should be useful in guiding towards the selection of a CE model having a good compromise between tractability and efficiency. A noticeable advantage of such improved CE descriptions would lie in the possibility of allowing more complex shapes for the free energy, in particular allowing several local minima, hence the possibility of simultaneous equilibria between a s.s. and several variants of the compound, a realistic situation which was excluded from the single-minimum IPDA carbide free energy described above.

In the present work, the equilibrium between the carbide and a HEA-type s.s. was investigated in a simplified manner, by considering that the chemical potentials of the metallic elements can be approximated by the energies of the pure elements with the same crystallographic structure (here bcc) as the s.s. Although a possibly crude approximation, it allowed us to enlighten interesting trends about the propensity of each metallic element of the s.s. to penetrate the carbide. More generally, our simplified scheme pointed out the importance of

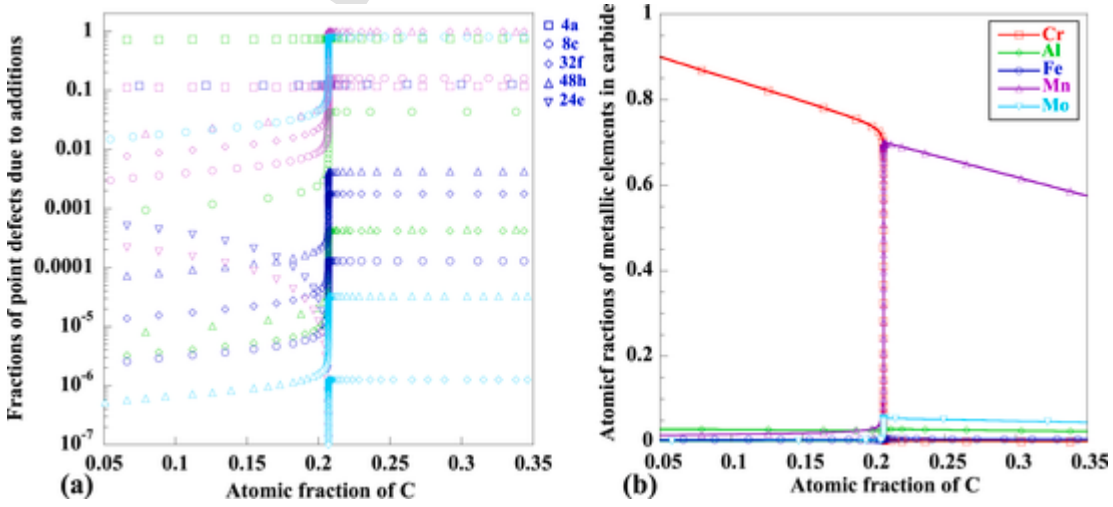

Fig. 5. Influence of the C content in $Cr_{23}C_6$ on the (a) amounts of substitutional addition metals (green, deep blue, purple and light blue are used for Al, Fe, Mn and Mo respectively, and the symbols refer to the various sublattices), (b) atomic fractions of metallic addition elements and Cr (red symbols for the latter), from ab initio IPDA thermodynamics, using for the chemical potentials of (Al, Fe, Mn, Mo) addition elements in the carbide, the values for these pure elements in the bcc structure (from Table 3).

the chemical potentials, which are the central quantities controlling the equilibrium trends. Starting from the atomic scale, the derivation of reliable evaluations for these composition-dependent quantities is a rather intricate issue. To this purpose, no privileged route seems to be currently available, and several competing approaches can be mentioned, in particular those relying on Special Quasirandom Structures (SQS) [24] or involving CE models [25,26]. While these routes should allow interesting refinements of the simplified estimation provided in our work, these approaches however have themselves intrinsic limitations, and therefore should probably be used in conjunction, in order to reach reliable chemical potentials. In particular, as already mentioned for carbides and other compounds, designing an accurate CE model for a multi-element s.s. constitutes a challenge in itself, and a compromise between simplicity and efficiency should be looked for, maybe by following a route similar to that previously used in slightly simpler situations, i.e. Al- and Mn-doped ferritic steels [19]. In such systems, the main hypothesis, strongly suggested by the chemical complexity, was to make use of CEs restricted to short-ranged pairs. In this context, the key-issue should thus be to derive ab initio-based pair interactions with sufficient reliability in the composition domain of interest. This task being probably much more difficult for HEAs than for steels, alternative approaches may also be employed to obtain such effective pair interactions, for instance those relying on first-principles high-throughput density functional theory calculations [27,28].

In the present study, most results were displayed as a function of the C content in the carbide, which was therefore considered as an independent variable. This is however an approximation, since the amounts of C, both in this phase and in a surrounding HEA s.s., are determined simultaneously by complex equilibrium conditions (equality of chemical potentials). Although estimating accurately the effective C content in the carbide is therefore a difficult task in the context of HEAs, an approximate analysis can however be carried out in the framework of our work: the latter provides a convenient picture in which the s.s. metallic chemical potentials can be seen as settled a priori, and then imposed "from outside" to the carbide phase. In particular, using the elemental energies in bcc structure as an approximation for the metallic chemical potentials in the s.s. obviously implies that the latter quantities are supposed to be independent of the amount of carbon in the s.s. Moreover, it should be noted that the dependence of the Cr and C chemical potentials on the carbide C content, as displayed on Fig. 4b for the case of "isolated" binary $Cr_{23}C_6$, was found not to be significantly modified when taking into account the other metallic elements with chemical potentials from Table 3 (i.e. the IPDA treatment leading to Fig. 5). Since the profiles of chemical potentials of Fig. 4b thus remain valid in presence of additional metallic elements, it is legitimate to report the energy of pure bcc Cr from Table 3 on this figure (green arrow), which gives an idea of the effective C content expected in the carbide surrounded by the AlCrFeMnMo HEA. It shows that, in this range of metallic chemical potentials, the bcc s.s. should act as a "buffer solution" for $Cr_{23}C_6$, since $\mu(Cr) = E_{bcc}(Cr)$ is found to lie within the zone of constant, roughly perfect stoichiometric, composition for the carbide. Nevertheless, since the width of the corresponding "stoichiometric window" for $\mu(Cr)$ is moderate (roughly 0.5 eV on Fig. 4b), easy shifts of the carbide C content towards either side of stoichiometry (either $> 6/29$ or $< 6/29$) cannot be excluded. Owing to Fig. 5b, this in turn suggests that a large uncertainty may subsist on the type of major metallic element, either Cr or Mn, really present in $Cr_{23}C_6$. Including carbon-metal interactions in the s.s. might be required to answer this question more precisely, as it would allow improving the approximation "$\mu = E_{bcc}$" used as input in the above IPDA treatment. On the whole, this emphasizes the importance of future theoretical and simulation works, in order to get a reliable atomic-scale description of the metallic chemical potentials in a HEA s.s., especially in presence of additional light elements.

5. Conclusion

Using ab initio-based energy properties and point-defect-based IPDA thermodynamics, we have provided an atomic-scale study of $Cr_{23}C_6$ carbides, these compounds being widely encountered in conventional alloys and recently detected in multimetallic concentrated AlCrFeMnMo bcc solid solutions typical of high-entropy alloys. We have shown that the properties of these carbides should be critically dependent on the role of interstitial carbon, which is unexpectedly found to occupy low-symmetry sites. Furthermore, the IPDA approach allowed us to explore the effect on $Cr_{23}C_6$ of the non-Cr metallic elements coming from the HEA-type environment. We evidenced the possibility of a competition between Cr and Mn, the latter element becoming possibly dominant in the carbide beyond a critical amount of C in the solid solution. To reach these conclusions, we adopted a simplified description by assimilating the metallic chemical potentials in the concentrated, roughly equimolar, AlCrFeMnMo solid solution to the energies of the corresponding pure bcc elements. While assessing the validity of this hypothesis should provide a topic for future works, it clearly demonstrates the interest of reliable and accurate atomic-scale schemes to reach the elemental chemical potentials in HEAs. The approach presented in this work may serve as a guide for (i) the selection of relevant more phenomenological thermodynamic models for ordered phases in equilibrium with concentrated multi-element solid solutions typical of HEAs, (ii) the interpretation of experimental measurements, e.g. in quantitative XRD analysis which requires delicate fits of diffraction profiles.

Declaration of Competing Interest

The author declares that he has no known competing financial interests or personal relationships that could have appeared to influence the work reported in this paper.

References

[1] C. Lee, Y. Chou, G. Kim, M.C. Gao, K. An, J. Brechtl, C. Zhang, W. Chen, J.D. Poplawsky, G. Song, Y. Ren, Y.-C. Chou, P.K. Liaw, Lattice-distortion-enhanced yield strength in a refractory high-entropy alloy, Adv. Mater. 32 (2020) 2004029.

[2] Y. Shi, B. Yang, X. Xie, J. Brechtl, K.A. Dahmen, P.K. Liaw, Corrosion of AlxCoCrFeNi high-entropy alloys: Al-content and potential scan-rate dependent pitting behavior, Corros. Sci. 119 (2017) 33–45.

[3] S.G. Ma, Creep resistance and strain-rate sensitivity of a CoCrFeNiAl0.3 high-entropy alloy by nanoindentation, Mater. Res. Express 6 (2019) 126508.

[4] T.S. Srivatsan, M. Gupta, High Entropy Alloys - Innovations, Advances, and Applications, CRC Press, 2020 (Editors).

[5] D.B. Miracle, O.N. Senkov, A critical review of high entropy alloys and related concepts, Acta Mater. 122 (2017) 448–511.

[6] O.N. Senkov, J.D. Miller, D.B. Miracle, C. Woodward, Accelerated exploration of multi-principal element alloys for structural applications, Calphad 50 (2015) 32–48.

[7] T. Stasiak, S.N. Kumaran, M. Touzin, F. Béclin, C. Cordier, Novel multicomponent powders from the AlCrFeMnMo family synthesized by mechanical alloying, Adv. Eng. Mater. 21 (5) (2019) 1900808.

[8] W.B. Pearson, P. Villars, L.D. Calvert, Handbook of crystallographic data for intermetallic phases, Am. Soc. Met. (1985).

[9] B.A. Senior, A critical review of precipitation behaviour in 1Cr-Mo-V rotor steels, Mater. Sci. Eng. A 103 (1988) 263–271.

[10] Y. Liao, R. Pourzal, P. Stemmer, M.A. Wimmer, J.J. Jacobs, A. Fischer, L.D. Marks, New insights into hard phases of CoCrMo metal-on-metal hip replacements, J. Mech. Behav. Biomed. Mater. 12 (2012) 39–49.

[11] C. Jiang, First-principles study of structural, elastic, and electronic properties of chromium carbides, Appl. Phys. Lett. 92 (2008) 041909.

[12] K.O.E. Henriksson, N. Sandberg, J. Wallenius, Carbides in stainless steels: results from ab initio investigations, Appl. Phys. Lett. 93 (2008) 191912.

[13] G. Kresse, J. Hafner, Ab initio molecular dynamics for liquid metals, Phys. Rev. B 47 (1993) 558–561.

[14] G. Kresse, D. Joubert, From ultrasoft pseudopotentials to the projector augmented-wave method, Phys. Rev. B 5 (1999) 1758–1775.

[15] J.P. Perdew, K. Burke, M. Ernzerhof, Generalized gradient approximation made simple, Phys. Rev. Lett. 77 (1996) 3865–3868.

[16] J.P. Perdew, K. Burke, M. Ernzerhof, Generalized gradient approximation made simple, Phys. Rev. Lett. 78 (1997) 1396-1396.

[17] H.J. Monkhorst, J.D. Pack, Special points for Brillouin-zone integrations, Phys. Rev. B 13 (1976) 5188–5192.
[18] M. Methfessel, A. Paxton, High-precision sampling for Brillouin-zone integration in metals, Phys. Rev. B 40 (1989) 3616–3621.
[19] R. Besson, J. Dequeker, L. Thuinet, A. Legris, Ab initio thermodynamics of complex alloys: the case of Al- and Mn-doped ferritic steels, Acta Mater. 169 (2019) 284–300.
[20] R. Besson, Point defects in multicomponent ordered alloys: methodological issues and working equations, Acta Mater. 58 (2010) 379–385. http://adpi.univ-lille1.fr/.
[21] K. Momma, F. Izumi, VESTA 3 for three-dimensional visualization of crystal, volumetric and morphology data, J. Appl. Crystallogr. 44 (2011) 1272–1276.
[22] R. Besson, Understanding phase equilibria in high-entropyalloys: I. Chemical potentials in concentrated solid solutions - Atomic-scaleinvestigation of AlCr-FeMnMo, to be published.
[23] R. Besson, R. Candela, Ab initio thermodynamics of fcc H-Zr and formation of hydrides, Comput. Mater. Sci. 114 (2016) 254–263.
[24] A. Zunger, S.H. Wei, L.G. Ferreira, J.E. Bernard, Special quasirandom structures, Phys. Rev. Lett. 65 (1990) 353–356.
[25] J.S. Wróbel, D. Nguyen-Manh, M.Y. Lavrentiev, M. Muzyk, S.L. Dudarev, Phase stability of ternary fcc and bcc Fe-Cr-Ni alloys, Phys. Rev. B 91 (31) (2015) 024108.
[26] D. Sobieraj, J.S. Wróbel, T. Rygier, K.J. Kurzydłowski, O. El Atwani, A. Devaraj, E. Martinez, D. Nguyen-Manh, Chemical short-range order in derivative Cr–Ta–Ti–V–W high entropy alloys from the first-principles thermodynamic study, Phys. Chem. Chem. Phys. 22 (2020) 23929–23951.
[27] M.C. Troparevsky, J.R. Morris, P.R.C. Kent, A.R. Lupini, G.M. Stocks, Criteria for predicting the formation of single-phase high-entropy alloys, Phys. Rev. X 5 (2015) 011041.
[28] L.J. Santodonato, P.K. Liaw, R.R. Unocic, H. Bei, J.R. Morris, Predictive multiphase evolution in Al-containing high-entropy alloys, Nat. Commun. 9 (2018) 4520.